The Institute of Space and Astronautical Science
Report No. 606, September 1983

Flow Visualization and LDV Measurement of Turbulent Mixing Layers

By

Osamu INOUE, Shun-itsu SATO and Hakuro OGUCHI

(August 27, 1983)

Summary: Structures of the turbulent mixing layers are experimentally investigated with special regard to its dependence on forced initial disturbances. The mixing layers are produced by setting a model screen perpendicular to the freestream at a test section. Initial disturbances are forcibly imposed by equipping with various sizes of a thin rod along the edge of the model screen or at the origin of the mixing layer. Fow features are observed by visualization technique by means of the smoke-wire method. Statistical quantities are measured by laser-Doppler velocimeter. Three kinds of model geometry are dealt with; these are of one-edged type, belt type, and circular disk type. The flows produced by these model screens represent, respectively, a plane mixing layer and two-dimensional and axisymmetric jets issuing into ambient stream of higher velocity. Fow visualization results indicate that the two-dimensionality of large-scale coherent structures seems to persist in high-turbulent flows, although comparatively smaller scale vortices are superimposed over the flow field within the mixing layer. The mixing layers are in self-preserving state, at least, up to third order moments, but in no universal state. The growth rates of the mixing layer are shown to strongly depend on the initial disturbance imposed.

Key Words: Mixing layer, Large-scale structure, Turbulence, LDV.

1. INTRODUCTION

Structures of turbulent mixing layers between two uniform flows of different velocity have been studied by many investigators, and various statistical quantities have been measured in detail mainly by means of hot-wire annemometers. It is now evident that the classical concept of turbulence, in which the properties of the various dynamic variables can only be determined in a statistical sense, is not quite complete. There are numerous evidences that at least in some cases turbulent flows are not so random as previously considered, but have some order in motion [1–3]. For example, Brown & Roshko [4] showed by flow visualization the presence of large-scale, quasi-ordered two-dimensional vortices in a fully turbulent two-dimensional mixing layer, and suggested that these quasi-ordered vortices may play an important role on the development of the shear layer. Winant & Browand [5] presented pictures which suggest that the amalgamation of neighboring vortices is one of the primary mechanisms responsible for the development of the shear layers.

A variety of studies on the mechanism or the structure of the turbulent mixing layer have been conducted both theoretically and experimentally, but there still remain many important questions to be answered. One of them is whether or not the self- preserv-

ing state of the turbulent mixing layer is dependent on the initial state of the flow. According to Townsend [6], self-preservation implies that primary statistical parameters of the flows are independent of the Reynolds number and become similar when they are rendered dimensionless through the characteristic velocity and length scale. It also implies that "a moving equilibrium is set in which conditions at the initiation of the flow are highly irrelevant". Recent data, however, cast some doubts on the universality of the concept of self-preservation. Wygnanski & Fiedler [7] experimentally studied the mixing layer in a half jet, which had been studied by Liepmann & Laufer [8]. The growth rate obtained by Wygnanski & Fiedler was approximately 30% larger than that obtained by Liepmann & Laufer. Batt [9] showed that a tripping wire placed on the splitter plate enhanced the growth rate of the mixing layer, and suggested that the difference of the growth rate between Liepmann & Laufer and Wygnanski & Fiedler may be mainly due to non-tripping or tripping the boundary layer on the splitter plate. He also suggested that an initial state of the shear layer may be a significant factor in determining the growth rate. Brown & Roshko [4] collected data given by various investigators for the growth rate of the mixing layer, and showed that there is a relatively large scatter among data. A variety of reasons have been proposed, but none is conclusive.

The two-dimensionality of the quasi-ordered vortices in an environment of high turbulence level is not universally accepted. Chandrsuda et al. [10] made flow-visualization and correlation measurements for the plane mixing layer, and showed that "Brown-Roshko structure" becomes highly three-dimensional when freestream turbulence level is high, or when the boundary-layer on the splitter plate is turbulent. They concluded, therefore, that the Brown-Roshko structure is rare in practice. On the other hand, Wygnanski et al. [11] studied the effects of external disturbances introduced into a mixing layer on the formation of large eddies, and showed that the two-dimensional character of the Brown-Roshko structure perseveres in spite of strong external disturbances. They concluded, in direct contradiction to that of Chandrsuda et al., that the Brown-Roshko structure is common in practice.

With these questions in mind, the present experiment was conducted to elucidate the structure of the turbulent mixing layers, especially, focusing on its dependence on forcible initial condition. In a conventional manner, the flow is separated into two streams of different velocity by using a splitter plate, and then fed to a test section. As suggested by Batt, however, the boundary-layer growing on the splitter plate seems to provide an appreciable influence on the development of the mixing layer. In this experiment, a mixing layer is produced by setting a model screen perpendicular to the freestream at the test section of the wind tunnel. The fluid passing through the model screen is decelerated, while the ambient fluid is accelerated. If the open-area ratio of the screen is suitably chosen, then both fluid flows may attain their respective uniform velocities shortly downstream from the screen. Three kinds of model geometry are employed; a wide or narrow screen fully spanned across the test section and a disk type of screen supported by a circular ring. The mixing layers produced by these model screens are regarded, respectively, as a plane mixing layer, and mixing layers of two-dimensional and axisymmetric jets issuing into the ambient stream of higher velocity. As for these

mixing layers, the effect of the initial disturbance on the development and structure is investigated by equipping with various sizes of a thin rod along the edge of the model screens. Qualitative features of the mixing layers are primarily observed by a visualization technique by means of the smoke-wire method. Statistical quantities of the fluctuating velocities are measured by using a laser-Doppler velocimeter (LDV).

2. Apparatus and Experimental Procedures

A photograph and a schematic diagram of the experimental apparatus are shown in Figs. 1 and 2, respectively. A low-speed wind tunnel of suck-down type was used. The test section was 1500 mm long, 330 mm high and 210 mm wide, being preceded by a nozzle of the contraction ratio 9:1. A honeycomb and three fine-mesh screens were installed in the nozzle. Windows of 270 mm high and 970 mm long are equipped on

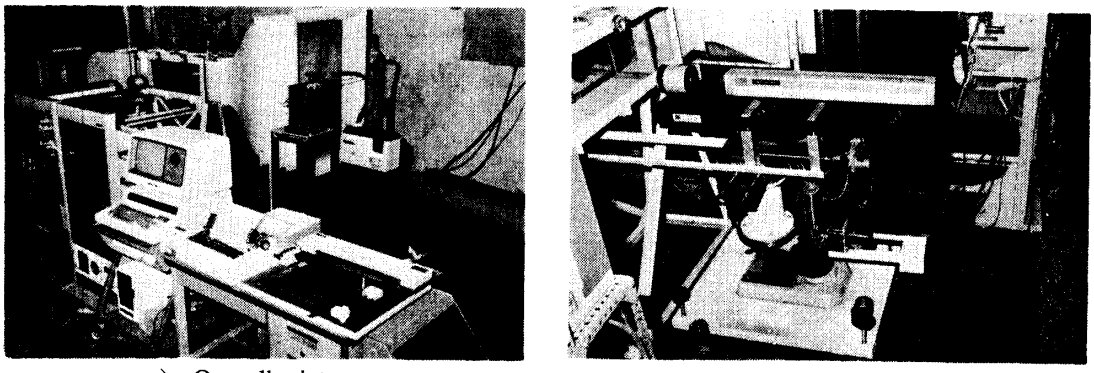

a) Overall picture b) LDV and traverse unit

Fig. 1. Photograph of experimental apparatus.

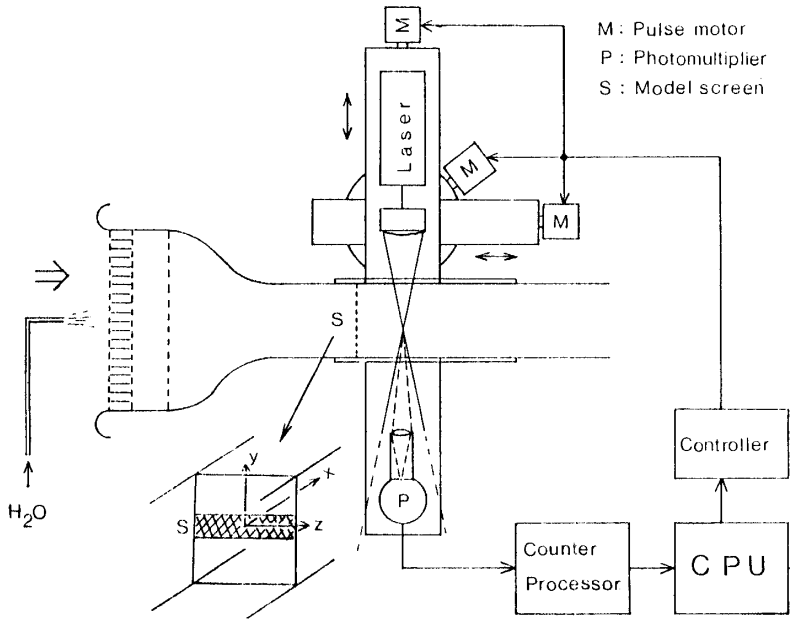

Fig. 2. Schematic diagram of experiment.

both sides of the test section, through which flow features are observed and also laser beams of LDV pass. The flow at the test section can be adjusted to any speed up to 15 m/s. In the experiment, the flow speed U_0 was chosen mostly at 3.2 m/s. The measured turbulence level was nearly 2%.

To realize the two streams of different velocity at the test section, a fine-mesh screen was set at the test section perpendicular to the freestream. Three kinds of the screen geometry were tested; one is a screen of 80 mm wide fully spanned across the test section (Case I), the second a screen of 32 mm wide also fully spanned (Case II), and the third a disk type of screen supported by a circular ring of 50 mm in diameter (Case III) (see Fig. 3). These screens were in 16 mesh weaved by 0.2 mm fine nylon wires (the open area ratio $\beta=0.764$). Let us suppose the flow around the model screens above mentioned. The freestream is decelerated after passing through the screen, while the ambient flow is accelerated downstream from the screen. These two streams may tend to attain their respective uniform velocities shortly downstream from the screen. This distance d, and the higher and lower stream velocities U_1, U_2 depend upon the blockage ratio of the model screen, the open area ratio of the screen, and the freestream velocity. Actually, these d, U_1, U_2 were measured for each model screen. For $U_0=3.2$ m/s and $\beta=0.764$, we obtained

for Case I: $U_1=3.63$ m/s, $U_2=2.50$ m/s, $d=40$ mm,
for Case II: $U_1=3.50$ m/s, $U_2=2.23$ m/s, $d=25$ mm,
for Case III: $U_1=3.38$ m/s, $U_2=2.15$ m/s, $d=25$ mm.

It was confirmed from these measurements that, in all cases tested, the two streams of nearly uniform different velocities are realized. This was also examined by the flow visualization by means of the smoke-wire method, shown later.

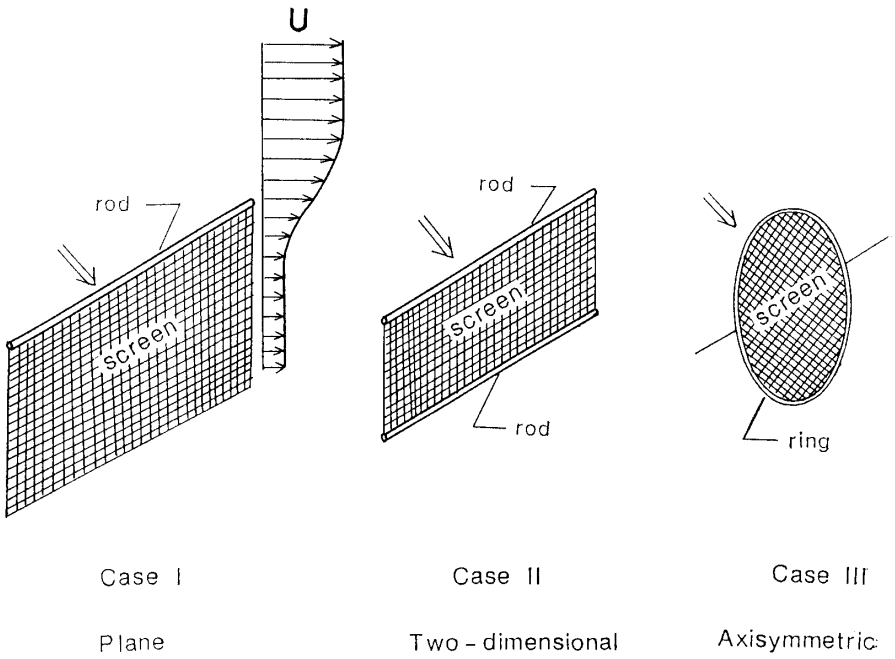

Fig. 3. The geometries of the model screen.

Next, let us suppose that a suitable size of rod is equipped with just along the edge of the screen (see Fig. 3). Such an equipment of rod imposes a forcible initial disturbance on the flow followed by the mixing layer. Apparently, the strength of the disturbance depends on the size of rod. In applying various sizes of rod and examining the resulting flow features, we may elucidate the effect of the forcible initial disturbance, thus imposed, on the development and the structure of the mixing layers, which are evolved after the model screens.

The flow features were observed by flow visualization by means of a smoke-wire method, using liquid paraffin. In applying the method, we used the smoke-wire with a number of knots, which enabled us to obtain a view of multiple, separate streaklines. The fine smoke-wire of 0.2 mm in diameter was spanned perpendicular to the freestream across the point 40 mm downstream from the screen. The photographs taken by flash covered a view in the streamwise distance x from the screen up to about 250 mm.

In addition to the flow visualization, the instantaneous velocities were measured over a region in question by means of a laser-Doppler velocimeter with He-Ne laser of the power 15 mW. By the photomultiplier detected was the forward scattering light from small seeded particles passing through the interference fringes caused by crossing two laser beams. The distance between neighbouring fringes was 3.18 μm and the angle between the two beams was 11.4°. In this experiment, the seeded particles were water vapour introduced just ahead of the honeycomb from a commercial humidifier. Both laser source and detector of the LDV were mounted on the same traverse unit, which was contrived to move precisely, by making use of a pulse motor (a stepping motor), in three orthogonal directions by a computer control. (See Figs. 1 and 2). The Doppler signals from the detector were stored on the disk of the computer through a counter processor (DISA 55L90).

The LDV was set such that the bisector of the crossing two beams is normal to the freestream at the test section. The Doppler signal can be deduced to the magnitude of the velocity component in the direction which agrees with the intersection of two-beam plane with the plane (x, y) normal to the bisector (see Fig. 2). For the two beams inclined anti-clockwisely by θ from the horizontal plane, the Doppler signal deduces the magnitude of velocity component:

$$|u\cdot\cos\theta+v\cdot\sin\theta|$$

where u, v are the velocity components, respectively, in the directions x and y. In this experiment, for one datum point $\theta=0°$, $\pm 45°$ were chosen, so that the laser singal for each angle deduced, respectively, $|u|$, $|u+v|/\sqrt{2}$, $|u-v|/\sqrt{2}$. Since $u \gg v$ over the flow field concerned, we can regard $|u|$, $|u+v|$, $|u-v|$, as u, $u+v$, $u-v$, respectively. At each angle θ, 3000 data per a datum point were read. From these 9000 data per a datum point the simple ansemble averages were evaluated by the following formula,

$$U=\bar{u},\ \overline{u'^2}=\overline{(u-U)^2},\ \overline{u'^3}=\overline{(u-U)^3},\ \overline{u'^4}=\overline{(u-U)^4}$$

$$\overline{v'^2}=[\overline{\{(u+v)-\overline{(u+v)}\}^2}+\overline{\{(u-v)-\overline{(u-v)}\}^2}]/2-\overline{u'^2}$$

$$\overline{u'v'}=[\{(u+v)-(u+v)\}^2-\{(u-v)-(u-v)\}^2]/4$$

$$\overline{u'v'^2}=[\{(u+v)-(u+v)\}^3+\{(u-v)-(u-v)\}^3]/6-u'^3/3$$

$$\overline{v'^3}+3\overline{u'^2v'}=[\{(u+v)+(u+v)\}^3-\{(u-v)-(u-v)\}^3]/2$$

where the primes denote the fluctuating velocity. Although the moments of u and u' can be derived up to any order as higher as desired, the moments with respect to v' are limited up to $\overline{u'v'^2}$ shown above. For derivation of higher order moments of v', data for the other angles θs are required. Measurements were made at 18 datum points across the mixing layer for several stations of x from 25 mm to 220 mm downstream from the model screen. The maximum of the Reynolds number U_1x/ν was 5×10^4.

In the LDV measurement of the mixing layer in a water channel, Dimotakis and Brown [12] reported the reproducibility as much as 5–10% for the mean velocity U. As they noted, the datum number of 1024 per a datum point in their experiment may not be large enough. In this experiment, the reproducibility is estimated less than 1.0% for the mean velocity U and 1.5% for the root-mean-square of the streamwise fluctuating velocity u'.

3. Results and discussion

3.1. *Results of flow visualization*

The photographs taken by the smoke-wire method for Case I at the freestream velocity $U_0=3.2$ m/s are shown in Fig. 4. The streamwise distance x up to about 250 mm is covered in the photograph. As mentioned before, the mixing layer in Case I is regarded as a plane mixing layer. Fig. 4(*a*) is for Case I with no forcible initial disturbance or no rod edged along the screen. The mixing layer is very thin and any large-scale structures do not yet grow in the view. The large-scale structures form further downstream. Quite a similar flow feature was seen for Case II.

As mentioned before, a rod was equipped with along the edge of the model screen in order to examine the effect of the initial disturbance on the development of the mixing layer. Various sizes of rod from 1 to 3 mm in diameter were employed. The sideviews of the flow are shown in Figs. 4(*b*)–(*d*) for Case I with variance of the size of the edged rod. It can be seen from these figures that the thicker rod or the stronger initial disturbance results in faster growth of the mixing layer, but the characteristic flow features are qualitatively similar to each other. The plan view of the same flow feature as that shown in Fig. 4(*d*) is presented in Fig. 4(*e*). For this case the smoke-wire was spanned parallel to the screen edge slightly above the center of the mixing layer.

There is some controversy concerning whether or not the two-dimensionality of the Brown-Roshko structure persists in an environment of high turbulence level. Brown & Roshko [4] and Wygnanski et al. [11] claimed the persistence based on the correlation measurements and visual observation, while Chandrsuda et al. [10] and Pui & Gartshore [13] denied it also based on the similar experiment. In the present experiment, the freestream turbulence level was approximately 2% at $U_0=3.2$ m/s, and was much higher than those in Brown & Roshko, Chandrsuda et al., Pui & Gartshore and Wygnan-

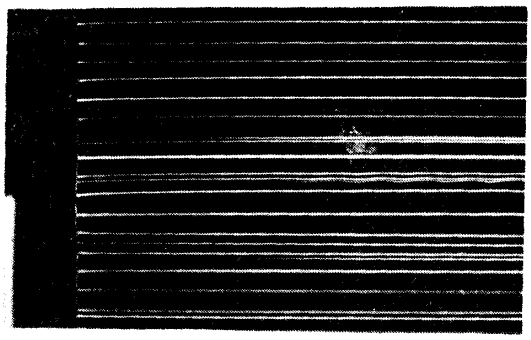

a) Side view. Without edged rod.

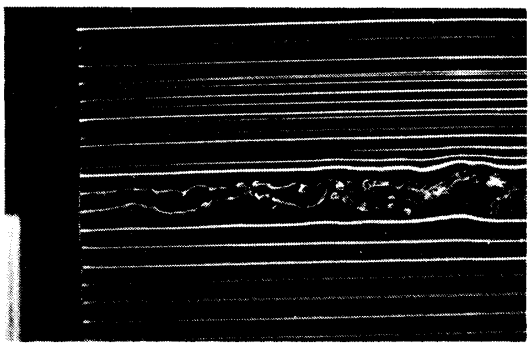

b) Side view. With 1 mm edged rod.

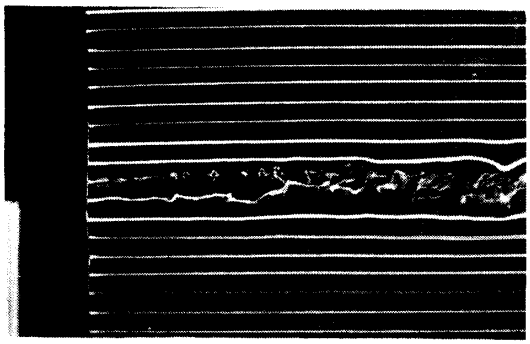

c) Side view. With 2 mm edged rod.

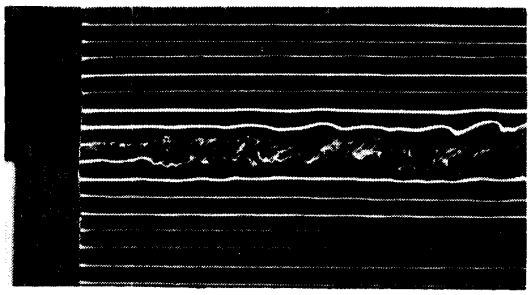

d) Side view. With 3 mm edged rod.

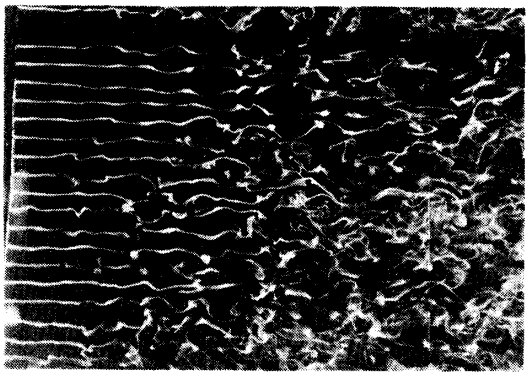

e) Plan view. With 3 mm edged rod.

Fig. 4. Photographs of the mixing layer for Case I. $U_0=3.2$ m/s.

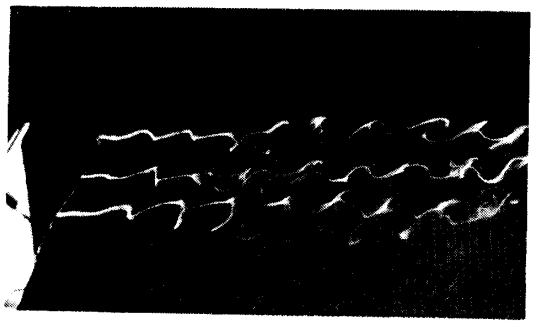

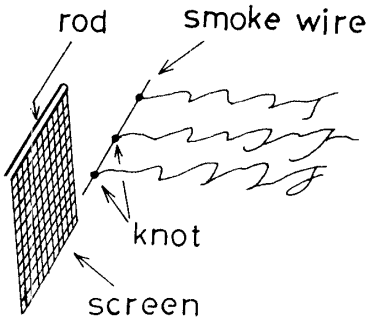

Fig. 5. Streaklines emanated from three positions along the z-axis. Case I. $U_0=0.8$ m/s. With 3 mm rod.

ski et al., but lower than that in the case (iv) of Wygnanski et al. The maximum Reynolds number in this experiment was 5×10^4 which is the lowest in all. For cases along with a forcible initial disturbance, the plan views as shown in Fig. 4(*e*) showed comparatively small-scale disturbances over the flow field within the mixing layer. On the other hand, the side views as shown in Fig. 4(*d*) showed somewhat coherrent, large-scale transverse vortices. Therefore, the two-dimensionality of the structure seems to persist as a whole, so far as the region in view is concerned.

In order to further confirm the two-dimensionality of the large scale structures, we set a smoke-wire with three knots parallel to the screen edge, say along the z-axis. The distance between neighboring two knots was about 40 mm. A photograph of the streaklines is presented in Fig. 5. Each perspective of the streaklines shown in Fig. 5 was transformed onto the respective x-y plane by means of a digitizer. The transformed streaklines shown in Fig. 6 may be regarded as their sideviews. It can be seen from Fig. 6 that large-scale structures within the mixing layer are nearly in phase. Thus, it is concluded that the two-dimensionality of the large-scale structures persists nearly in a highly turbulent flow, say turbulence level 2% in this experiment.

The photographs for Cases II and III, taken under the same condition as in Fig. 4 (*d*), are presented respectively in Figs. 7(*a*) and 7(*b*). The rods equipped with along the

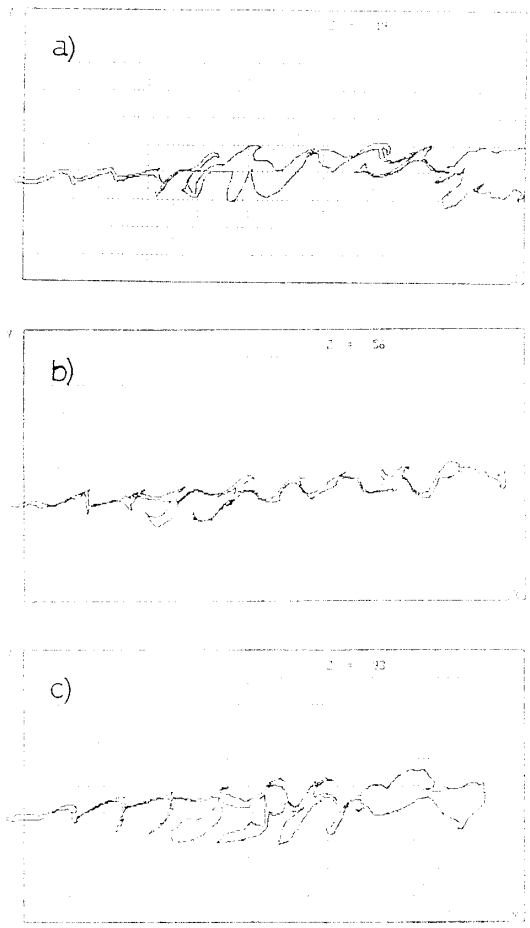

Fig. 6. Sideviews of the streaklines shown in Fig. 5.

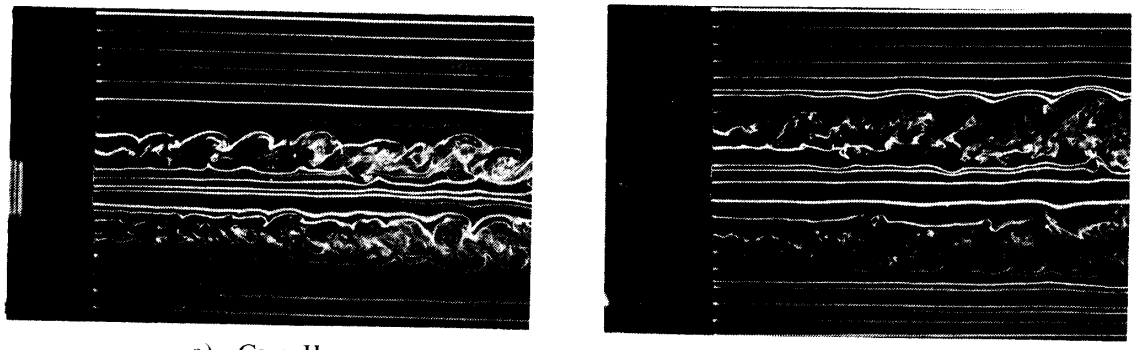

a) Case II b) Case III

Fig. 7. Side views of the mixing layer for Cases II and III. With 3 mm rod. $U_0=3.2$ m/s.

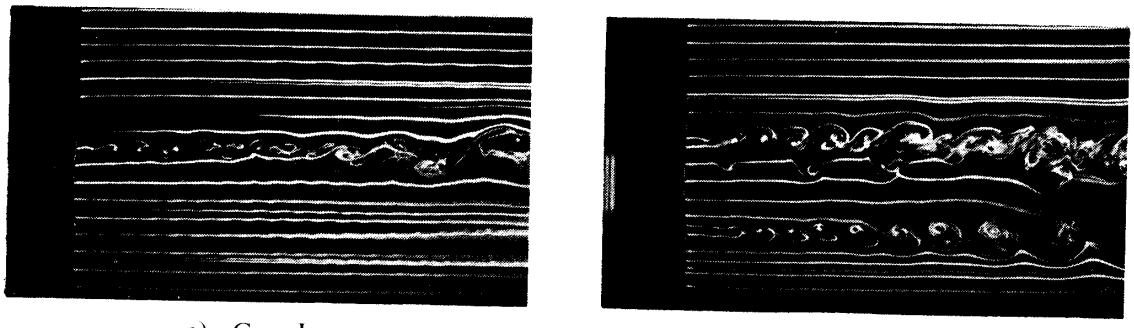

a) Case I. b) Case II.

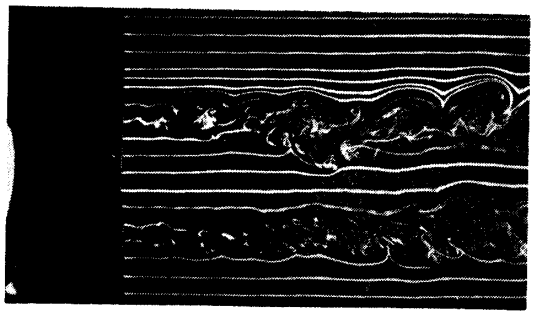

c) Case III.

Fig. 8. Side views of the mixing layer with slower freestream velocity. $U_0=1.6$ m/s. With 3 mm rod.

screen edge were 3 mm in diameter. Both upper and lower mixing layers do not closely interact with each other over the region covered in the photographs. It can also be seen from comparison with Fig. 4(*d*) for Case I that the characteristic features pertinent to the mixing layer are remarkably similar to each other among Cases I, II and III, in spite of the difference in both velocity ratio $r=U_2/U_1$ and type of the mixing layer. These characteristic flow features can more clearly be seen from the photographs in Fig. 8 taken at slower freestream velocities $U_0=1.6$ m/s. In Fig. 8 entrainment process is also clearly seen. The slower-speed fluid at the inner side region is entrained into the mixing layer faster than the higher-speed fluid at the outer side region. It results in that the mixing layer spreads more rapidly into the slower-speed flow region. It should be noticed from Fig. 8 that pairing vortices first reported by Winant & Browand [5] are

observed also in this experiment, and that vortex pairing process plays an important role in development of the mixing layer.

3.2. *Results of measurements by LDV.*

The measured region ($x=25$ mm to 220 mm) was roughly the same as that covered in the photographs presented in Figs. 4 and 7. All velocities are rendered dimensionless by the higher velocity U_1. The similarity coordinate η is defined as $\eta=(y-y_0)/x$ where the symbol y_0 denotes the y-component of a location where the mean velocity $U=(U_1+U_2)/2$ [7].

The profiles of the mean velocity and the fluctuating velocity components for Case I without forcible initial disturbance or without an edged rod are presented of the similarity form in Fig. 9. The mixing layer beyond $x=150$ mm is in a self-preserving state, as shown in the figure. As can be seen from Fig. 4(a) also, the width of the mxing layer

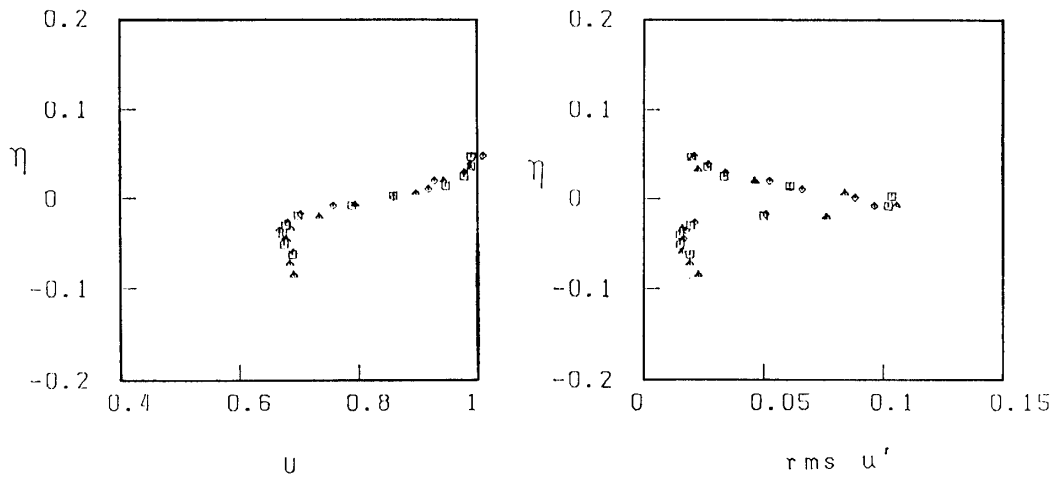

Fig. 9. Profiles of the mean and the fluctuating velocities for Case I. Without edged rod. $x=153$ mm; △, 183 mm; □, 217 mm; ◇.

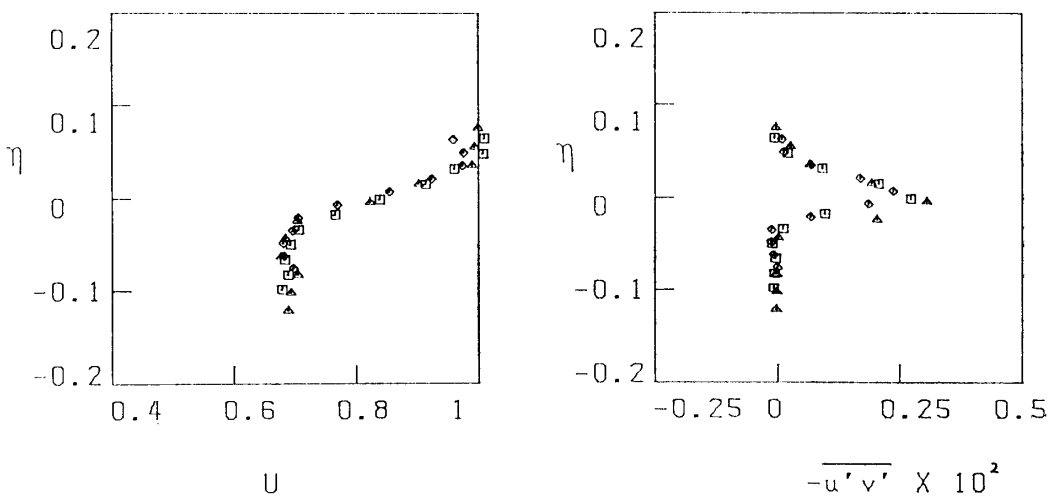

Fig. 10. Profiles for the mean velocity and the Reynolds stress for Case I. With 3 mm rod. (For legend, see Fig. 9.)

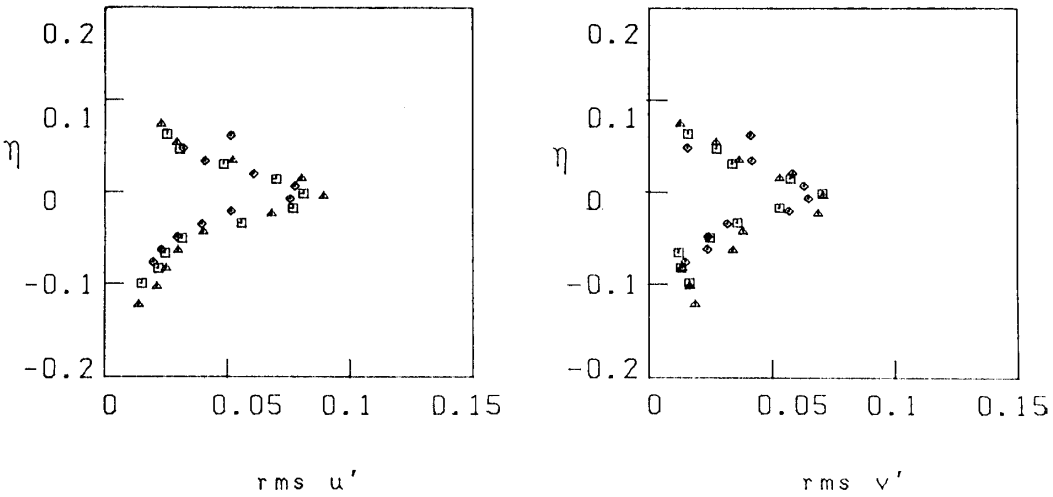

Fig. 11. Profiles for the r.m.s. component for Case I. With 3 mm rod. (For legend, see Fig. 9.)

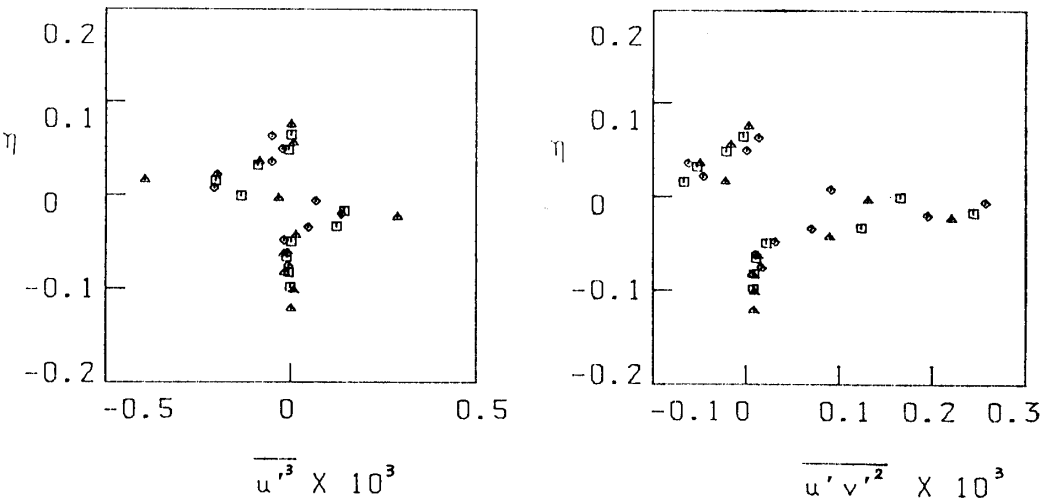

Fig. 12. Profiles for higher-order quantities for Case I. With 3 mm rod. (For legend, see Fig. 9).

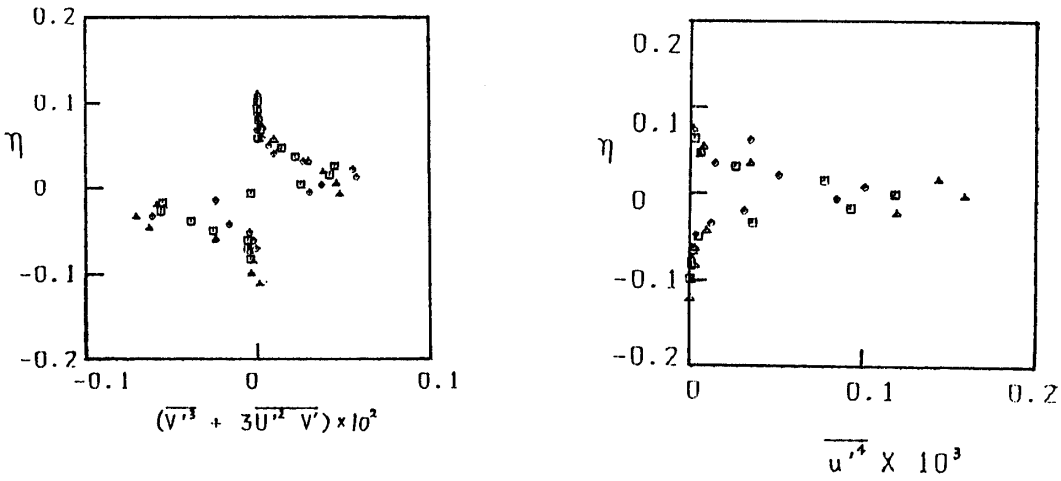

Fig. 13. Profiles for higher-order quantities for Case I. With 3 mm rod. (For legend, see Fig. 9).

is very thin. From these results, we can say that a relatively "clean" mixing layer is realized by setting a model screen at the test section.

The profiles of the statistical quantities up to the fourth order are shown in Figs. 10 to 13 for Case I along with an forcible initial disturbance by the equipment of 3 mm rod. It can be seen from these figures that all the statistical quantities shown are likely to be in a self-preserving state. The same can be seen from the results for Cases II and III (Figs. 14 and 15). From comparison between the cases with and without forcible initial disturbance, it can be seen that the structure of the disturbed mixing layer is different from that of the undisturbed mixing layer, though both flows are in their respective self-preserving states. This means that the memory of the initial disturbance persists in the self-preserving flows, and thus the flows are apparently not in an equilibrium self-preserving state discussed by Townsend [6]. Champagne et al. [15] noticed

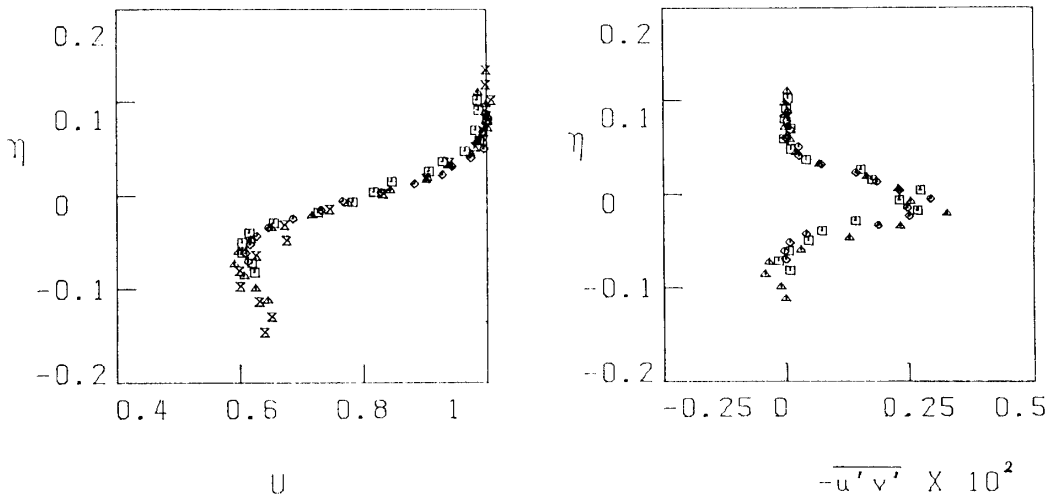

Fig. 14. Profiles of the mean velocity and the Reynolds stress for Case II. With 3 mm rod.

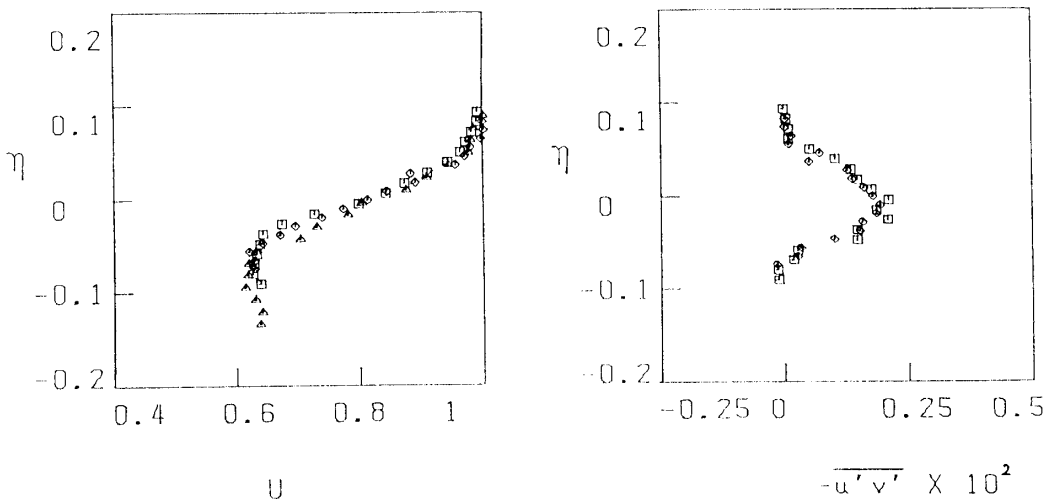

Fig. 15. Profiles of the mean velocity and the Reynolds stress for Case III. With 3 mm rod.

the importance of the disturbance level of the initial boundary-layer along the splitter plate in determining the growth rate and the maximum peak in the intensity profile of the fluctuating velocities. They suggested that no universal self-preserving form may exist; in other word, the self-preserving functions may depend on the initial conditions of the flow. This argument still holds for this experiment.

The relation between the growth of the mixing layer and the velocity ratio is customarily expressed as follows:

$$\delta_w/(x-x_0)=C\cdot(U_1-U_2)/(U_1+U_2)=C\cdot\lambda \qquad (1)$$

where δ_w is a representative width of a mixing layer defined by $\delta_w=(U_1-U_2)/(\partial U/\partial y)_{max}$ and x_0 is a virtual origin of the mixing layer. The growth rates obtained in the present experiment are listed in Table and also plotted versus λ in Fig. 16. Brown & Roshko [4] collected data obtained by various experiments and gave the value of the constant C equal to 0.181 as the best fit for the data, which is shown by the solid line in Fig. 16. They noticed, however, that there is a relatively large scatter among the data.

A variety of reasons for the scattering above mentioned has been presented; for example, the effect of the state of the initial boundary-layer on the splitter plate (Batt [9], Browand & Latigo [14], Champagne et al. [15]), the effect of the Reynolds number (Birch & Eggers [16]), the effect of the background frequency of the facility used (Weisbrot et al. [17], Pui & Gartshore [13]), turbulence in the free stream (Chandrsuda et al. [10], Pui & Gartshore [13]), and so on. It is generally accepted that the effect of the Reynolds number is secondary. Batt suggested, as already cited in the introduction, that the initial state of the mixing layer may be important in determining the

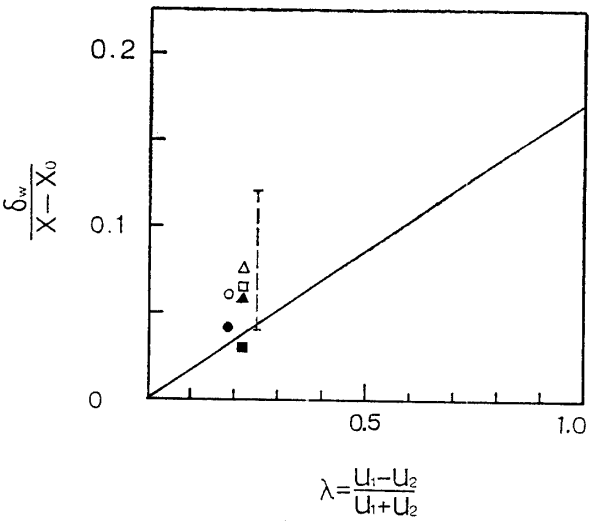

Fig. 16. The growth rates versus the speed ratio.
○: Case I (3 mm rod), ●: Case I (no rod),
□: Case II (3 mm rod), ■: Case II (no rod),
△: Case III (3 mm rod), ▲: Case III (1 mm rod),
——: Brown-Roshko [4], ·····: Weisbrot et al. [17]

Table of the growth rate and velocity ratio.

Case		$\lambda=\frac{u_1-u_2}{u_1+u_2}$	$r=\frac{u_2}{u_1}$	$\frac{\delta_w}{X-X_0}$	C
I	rod 3ϕ	0.183	0.69	0.060	0.328
	no rod	0.183	0.69	0.042	0.230
II	rod 3ϕ	0.220	0.64	0.064	0.291
	no rod	0.212	0.65	0.030	0.142
III	rod 3ϕ	0.220	0.64	0.075	0.341
	rod 1ϕ	0.220	0.64	0.058	0.264
Brown & Roshko					0.181

growth rate. The present results also more clearly show the importance of the effect of the initial state on the subsequent growth of the mixing layer; that is, in all three different geometries of the mixing layer, the larger initial disturbance leads the larger growth rate as can be seen from Fig. 16 and also Table. In Fig. 16, also plotted are the results of Weisbrot et al. In their experiment, for a fixed value of λ ($=0.25$), the growth rate varied with variance of the velocities U_1 and U_2. They attributed the reason to the background frequency of the facility used. The background frequency, however, may not neccessarily be a primary factor for the scatter of the growth rate. In fact, the present results showed different growth rates depending on the magnitude of the initial disturbance under the same background frequency or with the same tunnel operation. Quite recently Oster & Wygnanski [18] experimentally studied the effect of forced periodic disturbances, introduced at the initial stage of the mixing, on the subsequent development of the mixing layer. They found that the growth of mixing layer depends on both amplitude and frequency of the disturbance for the velocity ratio fixed. They concluded that the turbulent mixing layer depends on the initial conditions and therefore may never become a 'universal' self-preserving flow. The present experiment also shows qualitatively similar results to those of Oster & Wygnanski, although the initial disturbances were imposed in a way different from theirs.

4. Summary and Concluding Remarks

Relatively clean mixing layers were produced by setting a model screen at the test section. The structure of the mixing layer thus produced was investigated qualitatively by means of flow visualization and quantitatively by means of LDV. Special regard was paid to the effect of forcible initial disturbance on the development of the mixing layer. The initial disturbance was imposed by equipping with a thin rod along the screen edge or the origin of the mixing layer. Three different geometries of the mixing layer were dealt with; the plane mixing layer, and the two-dimensional and axisymmetric jets issued into ambient stream of higher velocity.

The flow visualizations lead that the two-dimensionality of large-scale transverse vortices appears to persist, as a whole, even in a highly turbulent flow (say, turbulence level 2% in this experiment), though comparatively small-scale disturbances are super-

imposed over the flow field in the mixing layer. Vortex pairing process was observed also in this experiment.

It was clearly shown that the initial disturbance has a significant influence on the development of the mixing layer; in any of three different geometries of the mixing layer, larger initial disturbance lead larger growth rate. The mixing layers dealt with in this experiment are in self-preserving state at least up to the third order. These self-preserving flows persevered memory of the initial conditions, so that there existed no universal self-preserving state.

References

[1] Laufer, J.: New trends in experimental turbulence research. Ann. Rev. Fluid Mech., Vol. 7, pp. 307–326, 1975.

[2] Cantwell, B. J.: Organized motion in turbulent shear flow. Ann. Rev. Fluid Mech., Vol. 13, pp. 457–515, 1981.

[3] Roshko, A.: Structure of turbulent shear flows: a new look. AIAA J., Vol. 14, pp. 1349–1357, 1976.

[4] Brown, G. L. & Roshko, A.: On density effects and large structures in turbulent mixing layers. J. Fluid Mech., Vol. 64, pp. 775–816, 1974.

[5] Winant, D. & Browand, F. K.: Vortex pairing: the mechanism of turbulent mixing-layer growth at moderate Reynolds number. J. Fluid Mech., Vol. 63, pp. 237–255, 1974.

[6] Townsend, A. A.: The Structure of Turbulent Shear Flows, 2nd edn. Cambridge University Press. 1976.

[7] Wygnanski, I. & Fiedler, H. E.: The two-dimensional mixing layer region. J. Fluid Mech., Vol. 41, pp. 327–361, 1970.

[8] Liepmann, H. W. & Laufer, J.: Investigation of free turbulent mixing. NACA TN No. 1257. 1947.

[9] Batt, R. G.: Some measurements on the effect of tripping the two-dimensional shear layer. AIAA J., Vol. 13, pp. 245–247. 1975.

[10] Chandrsuda, C., Mehta, R. D., Weir, A. D., & Bradshaw, P.: Effect of freestream turbulence on large structure in turbulent mixing layers. J. Fluid Mech., Vol. 85, pp. 693–704, 1978.

[11] Wygnanski, I., Oster, D., Fiedler, H. E. & Dziomba, B.: On the perseverance of a quasi-two-dimensional eddy-structure in a turbulent mixing layer. J. Fluid Mech., Vol. 93, pp. 325–335, 1979.

[12] Dimotakis, P. E. & Brown, G. L.: The mixing layer at high Reynolds number: large-structure dynamics and entrainment. J. Fluid Mech., Vol. 78, pp. 535–560, 1976.

[13] Pui, N. K. & Gartshore, I. S.: Measurement of the growth rate and structure in plane turbulent mixing layers. J. Fluid Mech., Vol. 91, pp. 111–130, 1979.

[14] Browand, F. K. & Latigo, B. O.: Growth of the two-dimensional mixing layer from a turbulent and nonturbulent boundary layer. Phys. Fluid, Vol. 22, pp. 1011–1019, 1979.

[15] Champagne, F. H., Pao, Y. H. & Wygnanski, I.: On the two-dimensional mixing region. J. Fluid Mech., Vol. 74, pp. 209–250, 1976.

[16] Birch, S. F. & Eggers, J. E.: NASA SP-321, 1973.

[17] Weisbrot, I., Einav, S. & Wygnanski, I.: The nonunique rate of spread of the two-dimensional mixing layer. Phys. Fluids, Vol. 25, pp. 1691–1693, 1982.

[18] Oster, D. & Wygnanski, I.: The forced mixing layer between pararell streams. J. Fluid Mech., Vol. 123, pp. 91–130, 1982.